

Imperial College London

MASTERS THESIS

OPTIMISING HUMAN-ROBOT INTERACTION USING ELECTROMYOGRAPHY AND ZERO-IMPEDANCE MODE - AN ASSISTED LOCOMOTION SCENARIO

Zoë Despature

Word Count: 5984

Supervised by:

Prof. Dr. Dario Farina

Dr. Hsien-Yung Huang

Department of Biomedical Engineering

June, 2021

Abstract

One of the challenges towards building wearable exoskeletons for rehabilitation and augmentation is that when fitted with an exoskeleton, a wearer will experience additional joint impedance around the knee due to the presence of the exoskeleton. To compensate for this additional joint impedance, zero-impedance control attempts to improve the dynamic response of an exoskeleton while giving the user full control priority, however resistance remains, arising from parameters specific to the coupled human-exoskeleton system. In this report, we propose an approach to parametric identification, identifying coupled impedance parameters in an effort to mathematically model a motion mismatch between a user and a knee orthosis. Our aim is to improve the dynamic response of the exoskeleton by taking into account un-identified features, without any previous knowledge of the control system. The approach taken uses electromyography (EMG) signals to estimate human joint torque, due to their widely acknowledged benefit of preceding the onset of movement. We show that the residual impedance between the human and the exoskeleton can be identified, capturing un-modelled characteristics with an accuracy up to 61.94%, averaging at 49.92%, based on the identification of coupled impedance parameters. We describe the experimental procedure, human subject testing with three healthy subjects, and data collection.

Acknowledgements

First and foremost, I would like to thank Professor Dario Farina, for inspiring an interest in the subject in his course "Digital Biosignal Processing", and for the opportunity to work in his research group for my masters thesis.

Of course, my completion of this project would not have been accomplished without the endless support of Dr. Hsien-Yung Huang, who made sure that I would always understand what I'm doing, and was an incredible mentor. I thank him very much for his precious time and valuable advice, both for this research and for the future.

Thank you to Shibo Jing, doctoral student in the Department of Mechanics, for generously offering time and help in the lab for the conduct of my experiments. I thank him for his patience and the time taken to make sure all my experiments were going well.

I would also like to thank Christopher Caulcrick for developing and providing the exoskeleton and computer interface used in this project.

Jonas Rauchhaus and Livia Robic gave their time to come to the lab and be the subjects of my experiments. I also take this opportunity to express my love and gratitude to my friends, without whom the past four years wouldn't have been anywhere near as fulfilling.

Last but definitely not least, I would like to thank my caring, loving and supporting family, for having supported me through all my years at Imperial College London. Their love and guidance in whatever I pursue have been my biggest motivation. I am infinitely grateful, and wouldn't be here without them.

Contents

| | |
|---|-----------|
| Abstract | i |
| Acknowledgements | ii |
| 1 Introduction | 1 |
| 1.1 Existing exo-skeletons and zero-impedance mode | 2 |
| 1.1.1 Model-based control | 2 |
| 1.1.2 Adaptive oscillators-based control | 2 |
| 1.1.3 Fuzzy control | 3 |
| 1.1.4 Sensitivity amplification | 3 |
| 1.2 Compensating unidentified features | 4 |
| 1.2.1 Adapting using machine learning | 4 |
| 1.2.2 Adapting using a control system | 4 |
| 1.3 Reverse-engineering approach to parameter identification | 5 |
| 1.4 Surface electromyography (sEMG) | 5 |
| 1.5 Aims and objectives | 6 |
| 2 Methods | 7 |
| 2.1 The human-exoskeleton system | 7 |
| 2.2 Equipment | 8 |
| 2.2.1 The Mechanical Engineering Department's exoskeleton | 8 |
| 2.2.2 Exoskeleton joint angle θ_e measurement | 9 |
| 2.2.3 Exoskeleton torque τ_e measurement | 9 |
| 2.2.4 Knee joint angle θ_k measurement | 10 |
| 2.2.5 Knee torque τ_k measurement | 11 |
| 2.3 Experimental protocol for parametric identification | 11 |
| 2.3.1 Identifying the exoskeleton gravitational torque $m_{e g l_e}$ | 11 |
| 2.3.2 Identifying the exoskeleton's response to torque input | 12 |
| 2.3.3 Identifying the human gravitational torque $m_{sh g l_{sh}}$ | 13 |
| 2.3.4 Identifying the knee torque τ_k | 14 |
| 2.3.5 Identifying the coupled inertia I_c , damping b_c and spring coefficients k_c | 14 |

| | |
|---|-----------|
| 3 Results | 15 |
| 3.1 Subjects | 15 |
| 3.2 Experimental results | 15 |
| 3.2.1 Identifying the exoskeleton's gravitational torque m_{egl_e} | 15 |
| 3.2.2 Identifying the exoskeleton's response to torque input | 16 |
| 3.2.3 Identifying the shank's gravitational torque $m_{sh}gl_{sh}$ | 17 |
| 3.2.4 Identifying the knee torque τ_k | 18 |
| 3.2.5 Identifying the coupled inertia I_c , damping b_c and spring coefficients k_c | 19 |
| 4 Discussion and conclusion | 21 |
| 4.1 Experimental results | 21 |
| 4.2 Conclusion and further work | 22 |

Chapter 1

Introduction

Exoskeletons can potentially assist patients with reduced mobility, to aid in rehabilitation [1] and to enhance our human capabilities [2]. For human performance augmentation, which this report will study, exoskeletons can reduce a wearer's effort when performing daily tasks while keeping their control capacities. However, a gap between human and computer must be bridged to fully realise the potential of such systems [3].

Human-robot interaction systems operating in unexpected environments are limited by their design, [4] e.g., due to the difficulty of effectively controlling faulty or unexpected behaviour. Synchronising with a human body is a particularly complex challenge to model or predict. Zero-impedance control is an assistive strategy utilized by active exoskeletons which aims at reducing the resistive force between a user and an exoskeleton to an ideal of zero. Any resistance picked up suggests a flaw which can be optimized, which therefore allows a good understanding of sub-optimalities within the control system. However, despite the many approaches that can be taken to achieve zero-impedance mode, a control system which encompasses all human behaviour can easily be too simple, or over-fitted, for the complex machine which is the human body. This un-identified impedance is due to human interaction being hard to predict, but also other factors adding to the complexity of implementing such a system. For example, limitations on weight, height, or other parameters to accommodate for different physical needs bring advantages when using a device on different subjects, but it also introduces new drawbacks given that different physical sizes and movement patterns will require a different response of the control algorithm [5]. Even when tailored to an individual, an exoskeleton control system will have to be compliant to different gait patterns throughout the day, or to more or less lose straps attaching the device to the user. On top of the control system being imperfect, these differences will add to the torque-mismatch between the user and the exoskeleton.

To tackle these imperfections, prediction of motion intention ahead of the movement is valuable. Muscle activity signals, such as electromyography (EMG) being generated prior to the movement onset [6], their monitoring allows for a potential prediction of an intended motion, and an adaptation of a system ahead of a movement. With appropriate signal processing, they can be used to represent joint torque to a reasonable accuracy. This can be further used as an indicator of torque mismatch between the human and the exoskeleton, signalling a flaw in the zero-impedance control system. Therefore, to address the problematic of this project, an EMG-based method allows to adjust the impedance of the exoskeleton while the subject is performing a movement, by identifying a torque mismatch and adjust the output position of the exoskeleton.

We propose an approach to impedance reduction of a one degree of freedom (1-DOF) knee exoskeleton supporting zero-impedance mode. The angular mismatch between a subject and an exoskeleton based on a torque input will be identified, and identifying coupled impedance parameters used to tune the gains of a control system. This tuned control system will then be useful to compensate the angular mismatch in real time, based on the torque input and on experimentally identified parameters proper to the subject.

This report will be organised as follows. Section 1 introduces existing exoskeletons implementing zero-impedance control, identifying flaws that arise and the efforts that have been made to optimise their output. A new approach to this optimisation problem is proposed, and a desired outcome is detailed. Section 2 describes the human-exoskeleton system, and outlines an experimental plan to identify coupled impedance parameters. Section 3 presents the experimental results and the outcome of the tuned control system. Finally, the results are discussed in Section 4, outlining research areas that can be addressed as a continuation of this project.

1.1 Existing exo-skeletons and zero-impedance mode

Across the literature, different assistive strategies were designed to try and predict human behaviour [7]. While each control strategy tackles the problem from a different angle, some flaws are left behind these control algorithms, leading to residual resistance against the human's desired movement. Here are some common control strategies that has been used in exoskeleton control:

1.1.1 Model-based control

A model based control strategy relies on a mathematical model deduced from a human-exoskeleton system. The activation of different daily life activities, such as walking, sit-to-stand or stand-to-sit, is usually triggered by a voluntary motion originating from a body part the user has control upon. For example, this trigger could be the press of a button.

HAL is a whole body exoskeleton developed by Japan's Tsukuba University and the robotics company Cyberdyne to help patients with different levels of paralysis [8]. When used to support paraplegic patients, the control strategy is based on a static human-HAL model. The intention of the user is communicated through a movement of their upper body, which triggers an assistance based on balance control and gravity compensation.

However, this control strategy relies on the accuracy of the model, which can sometimes be hard to approximate given the complexity of the system. Any un-modelled movement from the user would therefore be enough to create a resistance. It is therefore important to eliminate most of the unidentified characteristics during common dynamic conditions.

1.1.2 Adaptive oscillators-based control

This adaptive control method relies on the periodicity of the gait pattern of the patient. It uses the rhythmic property of locomotion gaits to deduce its own phase patterns in a coupled oscillatory network. The model synchronises with the frequency and phase of the periodic input signal of gait, which drives the exoskeleton's motion trajectory. This will allow to follow the user's intention.

The full body exoskeleton developed by T. Matsubara et al. implements an adaptive oscillators based control to assist healthy and weakened-muscle people for daily life walking [9]. The intention of this control system is to include the diversity of user motion, and to consider the interactions among a user, robot or environment.

This exoskeleton achieved a reduction of 40% in torque required by the user. In this case, the research team optimised this result by developing a fine-tuning algorithm, which takes into account the walking velocity of the user. However, this optimises the output of the control algorithm making small adjustments based on the specific walking pattern the user. Unknown behaviour will not be compensated by such a fine-tuning algorithm.

1.1.3 Fuzzy control

In a fuzzy-logic based control, inputs to the control system are passed into a decision interface, where human or experience based rules are inferred to produce an output. Fuzzy logic attempts to interpolate what the human response would be and fit the input to an intelligent output. This control method can be taken into consideration when an accurate dynamic model is difficult to identify. This controller is able to deal with imprecise signals in complex control situations. However, it has to be parameterized carefully since the output of the controller depends on the specific motion task being carried out, and on physical differences between users.

The lower limb exoskeleton developed by H. He et al. assists a physically weak person by processing their thigh elecromyography (EMG) data and passing them through a fuzzy controller [10]. This data was used to assist in movements such as sitting down, standing up, climbing stairs or squatting. It was experimentally tested on a healthy male and proved to be effective when comparing EMG signals while the exoskeleton was worn without and with assistance.

In this case, any unknown behaviour which causes a resistance between the user and the device will depend on the output of the fuzzy controller, and the way the boundaries to trigger each action is defined by the developer. This unknown behaviour will not be dependent of any parameters which can be measured from sensors, but on the boundaries set by the developer.

1.1.4 Sensitivity amplification

This control strategy relies on a positive feedback loop of the controller, amplifying the force exerted by the wearer on the exoskeleton. This control method is activated directly by the motions of the user. Ideally, this control method would predict the user's movements so perfectly that they wouldn't have to put any effort in their task.

The BLEEX is a lower extremity exoskeleton developed in the university of Berkeley [11]. The assistive strategy is based on sensitivity amplification controllers, where the gait phases are distinguished by foot insole sensors. It has allowed a user to carry a 34kg load while walking at 4.7km/h.

Un-modelled impedance can arise due to the straps coupling the human to the exoskelton, or to physical differences between subjects. This illustrates this projects aims, where the hypothesis is that these unidentified characteristics can be mathematically modeled.

To conclude on this section, different control systems can be employed to achieve a transparent and effective control. Note that this is not an exhaustive list of the control systems used for zero-impedance mode. An attempt was made in identifying the flaws in these control strategies, and where the residual

impedance can arise from.

1.2 Compensating unidentified features

The control strategies enumerated above pose a basis to an approach to zero impedance mode. However, despite accurate parametrization and modelling, some resistance remains between the user and the exoskeleton due to un-identified factors. These can arise due to physical differences between users or loose straps for example. A supplemental control system can therefore be developed in addition to the existing one, where, in a new scenario involving an exoskeleton operating under an unknown control system, an extra step is created to compensate resistance arising from unmodelled factors. It was noticed that in existing literature, minor components are commonly overlooked, such as straps, which results in motion mismatch. However, some research has been undertaken to tailor existing control systems and tackle sub-optimalities in a bottom-up fashion, detailed in the following subsections.

1.2.1 Adapting using machine learning

Machine learning can be a powerful tool when it comes to reducing un-identified impedance between a user and an exoskeleton. The algorithm will learn from the movements made by the user himself as he wears the device.

For example, HAL-5 is a Japanese exoskeleton which is designed for the physically weak, or for human augmentation [12]. The control of this exoskeleton is based on the monitoring of the surface electromyography (sEMG, detailed in Section 1.4) of the user, which gradually adapts to the gait pattern of the user. It learns as the user walks with the exoskeleton, and mimics his intentions based on previously executed tasks. The results achieved were optimal for each user and efficiently predicting their movements based on their own locomotion pattern, but only after 2 months of wearing the device [12].

NAEIES is another exoskeleton based on sensitivity amplification control, which was developed to carry heavy loads on different terrains [13]. This exoskeleton added a neural network to its control algorithm to compensate any non-zero steady state between the user and the device. This allows better shadowing of the human's intention, by tailoring the control system to the user.

Control using neural networks are used to approximate functions that are not obvious to the developer. The techniques used by the scientists above exploit the learning that can be done from the user's movement pattern. In fact, as discussed by Kurt Hornik in his paper [14], neural networks can be seen as universal approximators, using the abundance of data to give an output based on a machine learning algorithm. This universal approximator may however not be able to provide clear and physical meaning to all findings.

1.2.2 Adapting using a control system

While previously explored optimisation methods tackle the problem of fine-tuning a control system on an individual's gait pattern, some components remain overlooked, such as the tightness of the straps attaching the human to the exoskeleton. This factor is independent of a human's physical parameters, but hinders the optimal operation of the control system. In this project, we investigate a different approach to cancel the unidentified impedance, taking into account the above-mentioned interference. We look for a simple input to output relationship based on control theory, while tailoring the output to the user, and by exploiting our understanding of the system.

We hypothesise that the remaining impedance can be mathematically modelled with the help of parameters proper to the user. The coupled human-exoskeleton system will be described by a spring damper system, and the task will consist of identifying the parameters describing the model. Once a transfer function has been shaped, it will be fed into a control system such as a PID, which will then actively cancel the predicted remaining impedance. In [15], a similar control strategy approach was taken, however the gait phase detection was based on the ground reaction forces during the swing phase of gait. Here, the aim is to incorporate EMG in the control strategy, in order to benefit of the advanced prediction of human motion, and change the response of the system based on the gait phase and the current requirements of the user.

The hypothesis that the remaining impedance can be mathematically modelled leads to the task of understanding which parameter would be the most useful to measure with the available sensors (detailed in Section 2.2.1).

1.3 Reverse-engineering approach to parameter identification

A research group in the University of Sapienza, Rome, investigated a reverse engineering approach to identify the dynamic model used by a light weight manipulator with elastic joints, the KUKA LWR [16]. A procedure was set up to determine the value of coefficients imposed by the manufacturer, including the identification of joint stiffness.

This above mentioned study takes advantage of the information provided by the software interface of the robot, which outputs the link inertia matrix, the gravity vector (mass and coordinates of the center of mass of each joint), the link position and joint torque sensor data. Using an accurate equation of motion and relevant experiments, dynamic coefficients can be determined.

After deriving equation of motion of the coupled human-exoskeleton system, and with the use of in-built and added sensors in the exoskeleton, such a procedure can be implemented. This reverse-engineering approach to identify parameters proper to the human-exoskeleton system will help explore the hypothesis that remaining impedance can be modelled and actively canceled.

This project therefore needs to identify parameters such as stiffness of the joint and impedance during active control of the exoskeleton in order to determine if mathematical modelling of the existing control mismatch is feasible. Robotics engineering implements parameter-identification methods, and the methodology will base itself on what has been done in that field, applying it to the human body.

1.4 Surface electromyography (sEMG)

Electromyography signals (EMG) refer to the electric signals produced during muscle contraction, indicating the electrical activity of a muscle's motor units [17]. Two types of EMG signals can be identified: surface EMG and intramuscular EMG. Intramuscular EMG, while it is less noise-prone, is an invasive method. In this project, we are interested in the non-invasive approach to muscular activity recording, being sEMG. These surface-detected signals are useful to obtain information about the intensity of muscle activation, and most importantly, are generated prior to the motion intended by a human [18].

This type of signal is commonly used in exoskeleton assistive strategies [19]–[24]. In the context of zero-impedance control, EMG is often used as a torque prediction for human torque. For example, in [25], a method is presented to detect the intended motion using sEMG signals, showing that a leg orthosis can be controlled via calibrated sEMG signals. In [26], it is shown that sEMG is much more effective in predicting

human torque than mechanomyography (MMG), postulation used in [27] for human torque estimation prior to joint motions, allowing for advanced prediction of required output torque of a model predictive control architecture.

Therefore, in this scenario of zero-impedance control optimisation, prediction of human torque via sEMG signals is valuable for a real time adaptation of the designed control system . It will be used with appropriate signal processing, since sEMG is noise-prone [28]. This filtering method will be described in Section 2.

1.5 Aims and objectives

This research therefore aims to optimise the human-robot interaction between a user and an exoskeleton in the everyday scenario of locomotion. We will focus on the un-identified impedance between a user and his exoskeleton, which remains even in efficient control systems. The approach to impedance reduction proposed in this report is based on the identification of parameters proper to the human-exoskeleton system, used to determine the impedance components of unknown features creating resistance between the human and the exoskeleton. These parameters will describe the gains of a control system, compensating in real time the torque mismatch. We aim to use EMG signals for advanced prediction of human motion, allowing for the real-time reaction of the designed control system.

This approach has the advantage that it is adaptable to new users of an exoskeleton, through tuning of its parameters. When using zero-impedance mode, the addition of this step should compensate for unidentified impedance and allow for better control, such as a faster and less rigid response. It is also robust to new scenarios, new users, and different approaches to zero-impedance control, since it is solely based on the identification of parameters proper to the current coupled system. Therefore, under time varying conditions, this optimisation strategy ideally should synchronise the exoskeleton's torque profile with the motion intent of the user, in an effort to reduce human lower limb effort while walking with a wearable exoskeleton.

Chapter 2

Methods

2.1 The human-exoskeleton system

The system is modelled as a 1-DOF leg model, approximating the lower-leg swinging around the knee joint with locked-hip while the subject is standing (figure 2.1). The aim is to model the motion between the wearer's lower leg and the orthosis, assuming that the thigh stays perpendicular to the floor, and the shank is the only part in motion.

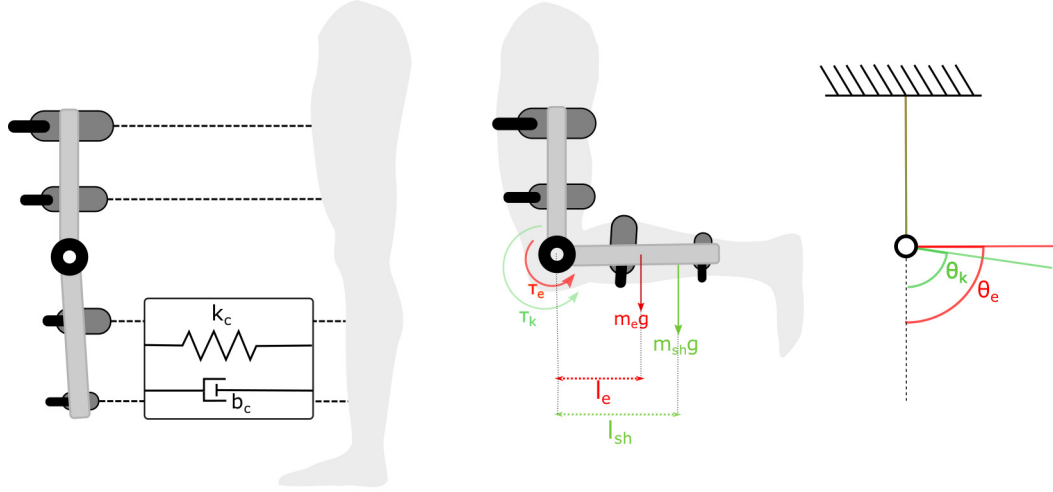


Figure 2.1: Free Body Diagram of the Human-Exoskeleton Model

During gait, the knee is estimated to provide a moment of inertia I_k , a damping coefficient b_k and a spring coefficient of k_k . Additionally, the exoskeleton has natural impedance parameters I_e , b_e and k_e , adding to the impedance parameters of the knee joint. The coupled system is therefore defined by a combination of these parameters, including unmodelled characteristics resulting in a coupled residual impedance. This is composed of the coupled moment of inertia, I_c , damping coefficient b_c , and elastic coefficient k_c . These parameters will guide an equation of motion, describing the dynamics of the human exoskeleton knee joint by the following system model:

$$\begin{aligned}
& I_k \ddot{\theta}_k(t) + b_k \dot{\theta}_k(t) + k_k \theta_k(t) \\
& + I_e \ddot{\theta}_e(t) + b_e \dot{\theta}_e(t) + k_e \theta_e(t) \\
& + I_c (\ddot{\theta}_k(t) - \ddot{\theta}_e(t)) + b_c (\dot{\theta}_k(t) - \dot{\theta}_e(t)) + k_c (\theta_k(t) - \theta_e(t)) \\
& = \tau_k + \tau_e - m_{sh} g l_{sh} \sin \theta_k(t) - m_e g l_e \sin \theta_e(t)
\end{aligned} \tag{2.1}$$

where:

- l_{sh} is the length of the shank-foot segment from the knee to the center of gravity of the lower leg
- m_{sh} is the mass of the shank-foot segment
- l_e is the length of the lower shaft of the exoskeleton
- m_e is the mass of the lower shaft of the exoskeleton
- $m_{sh} g l_{sh}$ describes the shank's gravitational torque
- $m_e g l_e$ describes the exoskeleton's gravitational torque
- θ_k is the knee angle (with angular velocity $\dot{\theta}_k$ and acceleration $\ddot{\theta}_k$)
- θ_e is the exoskeleton angle (with angular velocity $\dot{\theta}_e$ and acceleration $\ddot{\theta}_e$)

Since we model only the shank swinging around the knee, we assume that the weight of thigh segment of the exoskeleton is entirely withheld by the knee, without impacting the behaviour of the shank part of the exoskeleton. We also assume the inertia, damping and spring coefficients are constant. Knowing that the exoskeleton's control system does not overcompensate a torque mismatch, hitting the shank when a change in behaviour is noticed, the human and exoskeleton damping and spring coefficients can be neglected. Taking these assumptions into account, equation 2.1 can be simplified to:

$$\begin{aligned}
& I_c (\ddot{\theta}_k(t) - \ddot{\theta}_e(t)) + b_c (\dot{\theta}_k(t) - \dot{\theta}_e(t)) + k_c (\theta_k(t) - \theta_e(t)) \\
& = \tau_k + \tau_e - m_{sh} g l_{sh} \sin \theta_k(t) - m_e g l_e \sin \theta_e(t) - I_k \ddot{\theta}_k(t) - I_e \ddot{\theta}_e(t)
\end{aligned} \tag{2.2}$$

2.2 Equipment

2.2.1 The Mechanical Engineering Department's exoskeleton

An exoskeleton developed in the Mechanical Engineering Department of Imperial College London was lent for the purpose of this study. The 1-DOF knee-joint exoskeleton, which supports zero impedance mode, is made of a thigh and a shank segment (as pictured in figure 2.5). It is secured to the subject with four braces, which can be adjusted along a rail to fit subjects of different heights and weights.

The torque is delivered by a high power DC series elastic actuator (SEA), (HEBI, USA [29]), capable of communicating measurements on a GUI via an ethernet connection. The feedback is sent through an API in C++ controlling the actuator. This API enables real-time system state measurement, but also control of the actuator based on position, velocity or torque. The maximal output torque which can be safely delivered by the SEA is of 25Nm.



(a) Front view

(b) Side view

Figure 2.2: Pictures of the worn exoskeleton

The device is equipped with two high resolution incremental encoders on motor and joint sides, which accurately measure the output torque of the actuator based on the rotational deflection between the motor-side shaft and the output shaft. The sampling rate of the actuator is of 500Hz, and records the torque, the joint angle and angular velocity of the exoskeleton articulation. An IMU is also included in the actuator housing unit, monitoring the movement of the actuator.

2.2.2 Exoskeleton joint angle θ_e measurement

The two encoders included in the SEA , on the motor side shaft and the output shaft, record the position of both shafts. The feedback from the output shaft encoder is used in equation 2.2 as the exoskeleton joint angle θ_e . The angular velocity $\dot{\theta}_e$ and acceleration $\ddot{\theta}_e$ of the exoskeleton joint can be obtained by differentiation of the joint measurement.

2.2.3 Exoskeleton torque τ_e measurement

Figure 2.3 shows the actuator with the brushless motor encapsulating the encoders. Using the two encoders on the motor and joint side, the output torque of the actuator is measured based on the rotational deflection of the spring inside the actuator. This value is calculated using a calibrated spring constant in the actuator, and the rotational deflection between motor-side and output shaft. This will be used in equation 2.2 as the torque τ_e .



Figure 2.3: HEBI X-series actuator [29]

2.2.4 Knee joint angle θ_k measurement

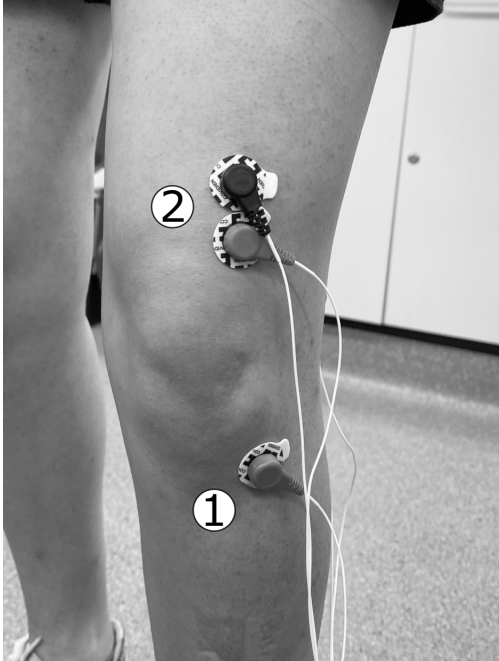
Since our aim is to identify a position mismatch, we use an external inertial measurement unit (IMU) to measure the human joint θ_k instead of the motor encoder. This IMU is secured on the ankle as shown in figure 2.4, to allow for a large range of motion while not being disturbed by the exoskeleton. We use an Arduino Nano 33 BLE [30], with an embedded 9 axis inertial sensor [31]. The acceleration, gyroscope and magnetometer data are fed into a Madgwick Filter [32] to provide position indications of the knee angle. To accurately estimate the knee angle based on the output of the Madgwick filter, the IMU is attached to the exoskeleton, and moved to different positions. The output of the Madgwick filter are then fed into a regression model to fit the recorded exoskeleton angle, providing a model capable of estimating the position of the human knee once attached to the ankle. The sampling rate of the IMU being 20Hz, an upsampling via interpolation is performed using MATLAB's `resample` function [33], to match the 500Hz sampling rate of the SEA.



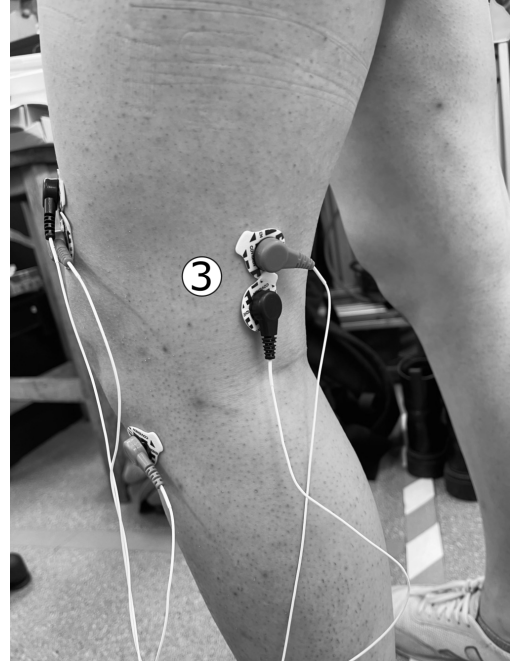
Figure 2.4: IMU placement

2.2.5 Knee torque τ_k measurement

The knee torque is estimated by mapping surface electromyographic (sEMG) data to the torque provided by the human using a regression algorithm. It is assumed that muscle activity signals are proportional to the force provided by the subject [34]. This relationship is exploited to estimate the knee torque τ_k . During gait, the rectus femoris (extensor) and the lateral hamstrings (flexor) are a pair of agonist antagonist acting at the knee joint [35]. This will guide the placement of the electrodes, as shown in figures 2.5a and 2.5b. The experimental procedure will be later described in section 2.3.4.



(a) Electrode placement on the rectus femoris



(b) Electrode placement on the lateral hamstring

Figure 2.5: EMG electrode placement (1) Ground electrode (2) Bipolar electrodes on the rectus femoris (3) Bipolar electrodes on the lateral hamstring

The EMG is picked up by bipolar electrodes (Covidien pre-gelled disposable electrodes), positioned according to the anatomical landmarks outlined in figures 2.5a and 2.5b. The signals are recorded and amplified using a TMSi Porti amplifier [36]. The EMG amplifier samples and filters signals at 2048 Hz, with corner frequencies of 10 Hz and 500 HZ, full-wave rectified, then lowpass filtered with a cutoff frequency of 2 Hz [37].

2.3 Experimental protocol for parametric identification

The variable measurement having been established above, the focus is now be brought on the identification of the constant parameters which remain un-identified in equation 2.2.

2.3.1 Identifying the exoskeleton gravitational torque m_{egl_e}

This step does not involve a human subject coupled to the system, and will therefore not involve recording of sEMG or IMU values. The exoskeleton is secured in an upright position as shown in figure 2.6, by securing

the thigh brace to a stable horizontal surface using a clamp. It is then controlled by a basic proportional controller from the GUI, and the angle θ_e and torque τ_e are recorded.

Given that $m_e g l_e$ is assumed to be constant, a static experiment is sufficient to identify the gravitational parameters. Therefore, in this scenario, equation 2.2 reduces to:

$$\tau_e = m_e g l_e \cos \theta_e. \quad (2.3)$$

Due to experimental imperfections, the static experiment will be performed at different angles in order to minimise error. The exoskeleton is therefore position-controlled, and held at angles in the range of $\theta_e = [0, 15, 30, 45, 60, 90]$ degrees for 5 seconds to capture the steady state response. The gravitational parameters are identified by fitting a linear trend line to the torque data plotted against the angle using MATLAB's `polyfit` function, which approximates coefficients of a line that best fit the data in a least-squares sense [38].



Figure 2.6: Experimental setup for gravitational torque identification

2.3.2 Identifying the exoskeleton's response to torque input

The aim is to identify the transfer function, estimated to have two poles and no zeroes, of the exoskeleton's response to a torque input in order to determine the control output and the natural impedance parameters of the exoskeleton. A recursive least-squares approach is taken for the identification of the parameters, using MATLAB's `system identification` toolbox to estimate a 2 poles and no zeroes transfer function expressed as:

$$\frac{\theta_e}{\tau_e} = \frac{1}{I_e s^2 + b_e s + k_c} \quad (2.4)$$

The exoskeleton is kept in the same configuration as in the experiment described in Section 2.3.1. It is instructed to output a sinusoidal trajectory with varying frequencies corresponding to usual walking frequency. For a normal gait, these will go up to 2Hz [39]. Given that a subject equipped with an exoskeleton will walk slower than usual, we choose to input frequencies in the range of $f = [0.3, 0.5, 0.7, 1]$ Hz. The input



Figure 2.7: Ridig plaque replacing the exoskeleton straps (1)

torque will have a defined amplitude of 1 rad, corresponding to the maximum angle during the swing phase of the gait cycle [40]. The target movement profile is therefore defined by:

$$\theta_e = \sin(2\pi ft) \quad (2.5)$$

where f is the input frequency and t is the time in seconds.

The output torque τ_e and joint angle θ_e are monitored. Each torque frequency is input for 5 seconds, enough to capture the steady-state behaviour of the exoskeleton once in action. The recorded data will be fed into a system identification algorithm to identify the exoskeleton's natural impedance parameters I_e , b_e and k_c .

2.3.3 Identifying the human gravitational torque $m_{sh}gl_{sh}$

The human gravitational parameters $m_{sh}gl_{sh}$ can be inferred using the exoskeleton parameters determined in the experiment above and the model outlined in equation 2.2.

In order to cancel the elastic and damping coefficients k_c and b_c , the exoskeleton is coupled to the human via a rigid link, replacing the soft straps with a rigid plaque to fix the exoskeleton to the leg as shown in figure 2.7. The static nature of experiments also cancels the angular acceleration and velocity terms $\ddot{\theta}_e$, $\dot{\theta}_k$, $\ddot{\theta}_e$ and $\dot{\theta}_k$. The subject is then asked to stay relaxed, to produce no knee torque τ_k . This will be monitored via EMG recordings. Equation 2.2 therefore reduces to:

$$\tau_e = -m_{sh}gl_{sh} \cos \theta_k - m_e g l_e \cos \theta_e \quad (2.6)$$

The exoskeleton is position controlled, and instructed to hold the shank at an angle $\theta_e = [0, 15, 30, 45, 60, 90]$ degrees to get multiple data points and reduce error. Each exercise will be 5 seconds long in order to limit subject discomfort, and three trials will be carried out.

The output torque is monitored, and using the previously identified constants, equation 2.6 is solved for $m_{sh}gl_{sh}$.

2.3.4 Identifying the knee torque τ_k

As explained in Section 2.2.5, the knee torque is identified by creating a mapping from sEMG data to the knee torque. After connecting the EMG electrodes [36], the knee orthosis is secured to the subject with the braces. The subject is asked to hold his lower leg angles $\theta_k = [0, 15, 30, 45, 60, 90]$ degrees, achieved by looking at the current encoder angle in the computational interface. Once the angle is reached, the exoskeleton initiates a torque-control. For each angle, the subject is asked to counteract a torque which is input from the exoskeleton's GUI. The torques gradually increments, from 0, to 5, to 10N, taking human fatigue into account. Each step lasts 5 seconds, and three trials are carried out. The knee angle is monitored to be taken into account in the mapping model, as it is unstable due to the human counteracting a torque. With this data, a regression model is fitted, and the human torque is deduced from the EMG readings.

2.3.5 Identifying the coupled inertia I_c , damping b_c and spring coefficients k_c

In equation 2.2, the coupled inertia, damping, and spring coefficients I_c , b_c and k_c still require identification. The subject coupled to the exoskeleton with the straps, and the assistive strategy is set to zero-impedance mode. The subject swings his shank, while the exoskeleton torque τ_e and angle θ_e , and human torque τ_k and angle θ_k are monitored. Using the m_{egle} and m_{shglsh} parameters identified in the previous experiments, equation 2.2 can be solved using a least squares approach.

We assume the impedance to be modelled by a transfer function with two poles and no zeroes, expressed as:

$$\frac{\theta(s)}{\tau(s)} = \frac{1}{I_c s^2 + b_c s^2 + k_c} \quad (2.7)$$

where I_c , b_c and k_c are the coupled inertia, damping and spring coefficients respectively. This transfer function will be identified using MATLAB's **system identification** toolbox [41]. This toolbox estimates model parameters using measurements of the input and output signals of a system. We will therefore feed torque data as input to the toolbox, and some angular data as the output. Given the condition that the transfer function has to have two poles and no zeroes, the model parameters are estimated by minimizing the error between the model output and the measured response.

Chapter 3

Results

3.1 Subjects

The experiments were carried out with three subjects, all healthy with no known physical injury on the knee joint. Subject information is provided in table 3.1, alongside the measured shank length l_{sh} from the knee to the heel. All subjects were given an experimental protocol and were able to follow the instructions.

Table 3.1: Subject information

| | Subject 1 | Subject 2 | Subject 3 |
|---------------------|-----------|-----------|-----------|
| Sex | Female | Male | Female |
| Age | 21 | 23 | 21 |
| Weight (in kg) | 54 | 68 | 52 |
| Height (in m) | 1.63 | 1.78 | 1.62 |
| Shank length (in m) | 0.42 | 0.55 | 0.46 |

3.2 Experimental results

3.2.1 Identifying the exoskeleton's gravitational torque $m_e g l_e$

The experiment outlined in section 2.3.1 is carried out, torque and angular data is collected, and a linear trend line is fitted as shown in figure 3.1.

Solving equation 2.3, the gravitational torque is deduced and shown in table 3.2 alongside the theoretically estimated torque. The center of mass of the shank part of the exoskeleton is assumed to be located mid-way of the segment.

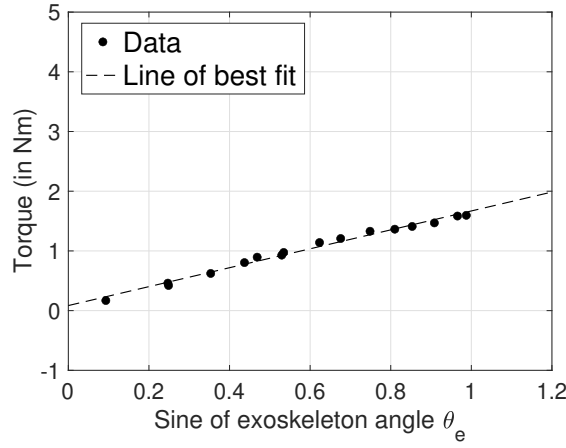


Figure 3.1: Line of best fit for data collected in Experiment 1

3.2.2 Identifying the exoskeleton's response to torque input

The experiments described in Section 2.3.2 are carried out. The exoskeleton torque τ_e and angle θ_e are monitored, and the transfer system described in equation 2.4 is solved, taking the torque as an input, and the angle as an output. The response of the identified system to a torque input of frequency 0.7 is shown in figure 3.2.

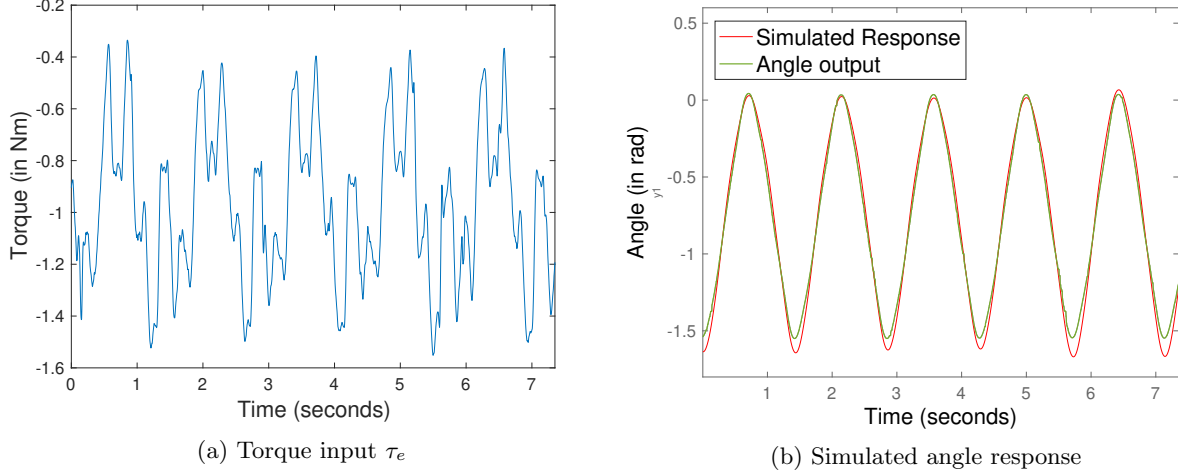


Figure 3.2: Simulated response of exoskeleton to torque input

The identified transfer function yields a 92.02% fit to the estimation angular data. The deduced impedance parameters can be referred to in table 3.2. A theoretical value is also computed, making the assumption that the shank segment of the exoskeleton can be approximated to a rod, using the following equation:

$$I_e = \frac{1}{3} m_e l_e^2 \quad (3.1)$$

Table 3.2: Theoretical and experimentally identified exoskeleton parameters

| | Theoretical | Experimental |
|--------------------------------|-------------|--------------|
| m_e (in kg) | 0.74 | |
| l_e (in kg) | 0.21 | |
| $m_e g l_e$ (in Nm) | 1.524 | 1.584 |
| I_e (in kg.m^{-2}) | 0.0435 | 0.0484 |
| b_e (in Ns.m^{-1}) | | 0.0083 |
| k_c (in N.m^{-1}) | | 1.2859 |

3.2.3 Identifying the shank's gravitational torque $m_{sh} g l_{sh}$

Following the experimental procedure described in Section 2.3.3, we collect torque and angular data, as plotted in figure 3.3.

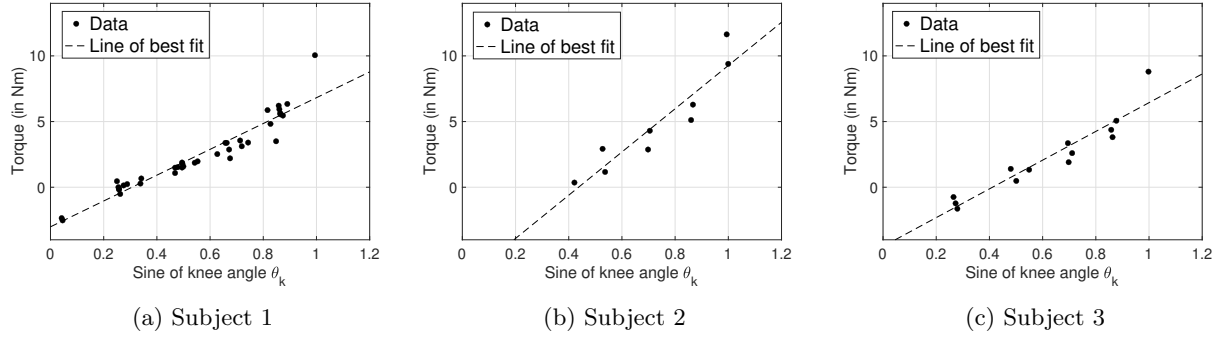


Figure 3.3: Collected data and line of best fit for shank gravitational torque identification

Using the mathematical expression of the line of best fit, the experimental values of the gravitational torque of the lower leg are deduced, and shown in table 3.3.

According to David A. Winter's Biomechanics and Motor Control of Human Movement [18], the lower leg's mass represents 6.1% of the total body weight m . Moreover, the center of mass of the lower leg is located at 60.6% of the total lower leg's length l from the knee. Therefore:

$$\begin{aligned} m_{sh} &= 0.061 \times m \\ l_{sh} &= 0.606 \times l \end{aligned} \tag{3.2}$$

We compare the theoretical and the experimental values in table 3.3.

Table 3.3: Theoretical and experimentally identified human parameters

| | | Subject 1 | Subject 2 | Subject 3 |
|--------------|---|-----------|-----------|-----------|
| Theoretical | m_{sh} (in kg) | 3.294 | 4.148 | 3.172 |
| | l_{sh} (in m) | 0.2545 | 0.333 | 0.2788 |
| | I_k (in $\text{kg} \cdot \text{m}^{-2}$) | 0.345 | 0.6771 | 0.363 |
| | $m_{sh}gl_{sh}$ (in Nm) | 8.225 | 13.56 | 8.674 |
| Experimental | $m_{sh}gl_{sh}$ (in Nm) | 8.244 | 14.87 | 9.355 |

3.2.4 Identifying the knee torque τ_k

The experimental setup outlined in Section 2.3.4 is carried out. The most efficient mapping method was determined to be an ensemble regression algorithm with least-squares boosting [42]. This model was trained using MATLAB’s `fitrensemble` function. A comparison of the performance of different regression algorithm is shown in table 3.4.

Ensemble regression is based on the combination of prediction from multiple models, and least squares boosting optimises the output using the difference between the observed response during training, and the aggregated prediction of all learners previously grown. The output of the regression algorithm is smoothed over 25 samples (equivalent to 50ms). The estimated human torque during a flexion movement is shown in figure 3.4 alongside the torque provided by the exoskeleton.

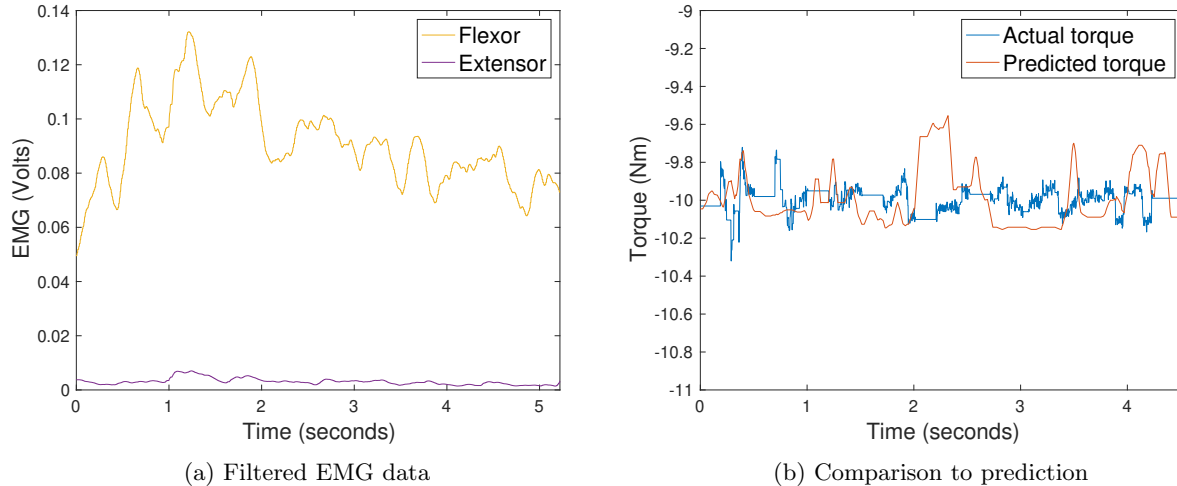


Figure 3.4: Human torque estimated from EMG data using an ensemble regression algorithm. Exoskeleton was providing a torque of 10Nm at an angle of 15 degrees.

Table 3.4: Regression algorithm performance

| | Ensemble with LS Boost | Ensemble with Bagging ¹ | Tree |
|--------------|---------------------------|---------------------------------------|-------|
| RMSE (in Nm) | 0.9554 | 0.999 | 2.114 |

3.2.5 Identifying the coupled inertia I_c , damping b_c and spring coefficients k_c

The inertia of the shank is theoretically calculated as in equation 3.3 (taken from [18] and the subject measurements from table 3.3), and is reported for each subject in table 3.3.

$$\begin{aligned} I_k &= I_0 + mx^2 \\ &= m\rho_0^2 + mx^2 \end{aligned} \tag{3.3}$$

The governing dynamical equation derived in Section 2.1 is then solved. Using MATLAB's `system identification` toolbox (described in Section 2.3.5), the transfer function is estimated. The comparison between the actual angle difference and the simulated angle difference are shown in figures 3.5b, 3.6b and 3.7b.

The simulations fit the estimation data with an accuracy averaging 49.92%, with a RMSE of 0.075 rad on average. The identified impedance parameters are reported in table 3.5. The results will be discussed in the next Section (Discussion, Section 4), also addressing experimental flaws explaining statistical outliers.

Table 3.5: Identified coupled parameters

| | Subject 1 | Subject 2 | Subject 3 |
|--------------------------------|-----------|------------|-----------|
| I_c (in kg.m ⁻²) | 0.0609 | 0.7536 | 0.1540 |
| b_c (in Ns.m ⁻¹) | 0.7870 | 2.7569e-09 | 0.2187 |
| k_c (in N.m ⁻¹) | 4.1411 | 20.9489 | 3.5228 |
| Fit to estimation data (in %) | 57.8 | 61.94 | 30.15 |
| RMSE (in rad) | 0.1297 | 0.0338 | 0.06134 |

¹Bootstrap Aggregation [42]

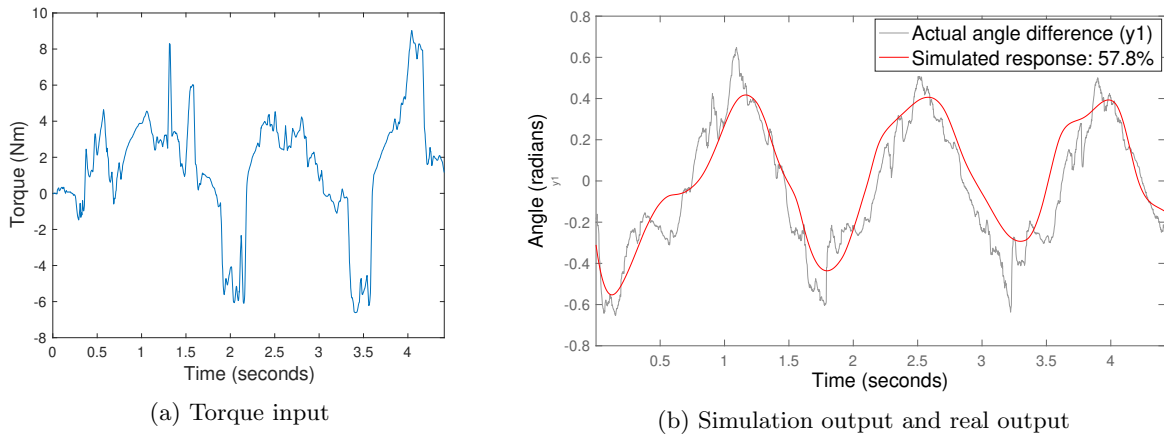


Figure 3.5: System identification for Subject 1

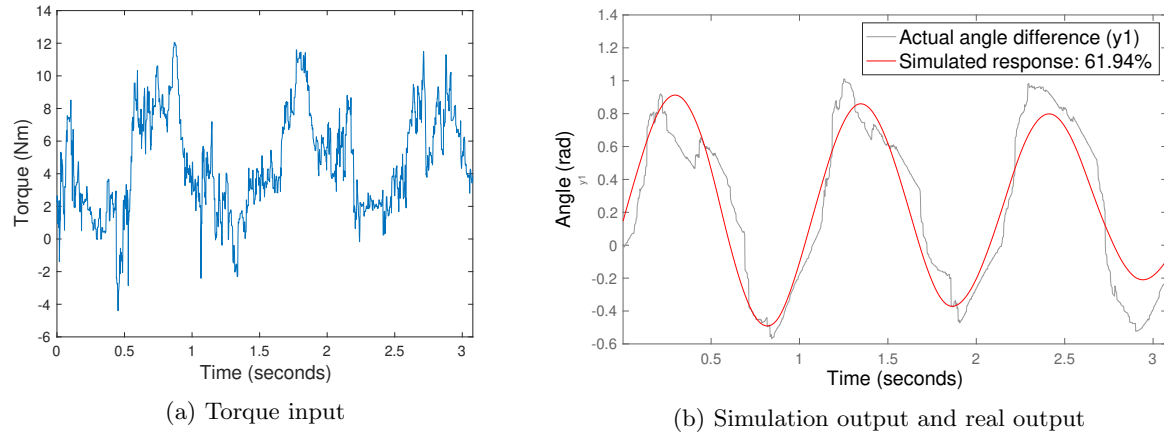


Figure 3.6: System identification for Subject 2

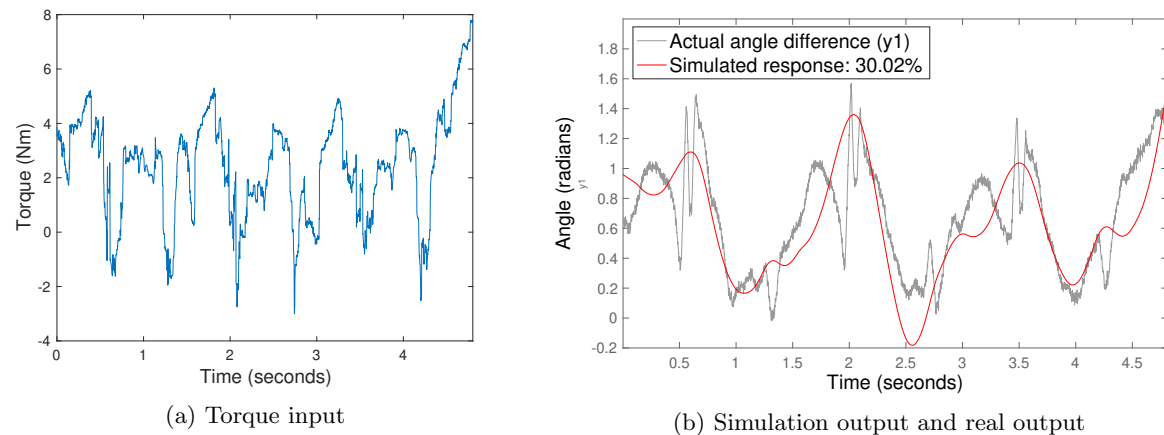


Figure 3.7: System identification for Subject 3

Chapter 4

Discussion and conclusion

4.1 Experimental results

The results show that physical constants can be experimentally identified to a high accuracy. The gravitational torques of the exoskeleton and shank have been identified with 96.21% and a 94.56% accuracy respectively for the three subjects. Using a system identification method to deduce the exoskeleton's natural impedance parameters, it has been shown that this impedance can be experimentally deduced with 89.88% accuracy relative to the theoretical values. The knee torque was estimated using sEMG signals, with an ensemble regression algorithm estimating the human knee joint torque with a RMSE of 0.9554Nm.

Regarding the identification of the coupled impedance terms, note that the impedance parameters for subject 2 are statistically anomalous relative to the other subjects, with little physical meaning to such high inertia. This indicates experimental error due to the Arduino IMU experiencing sensor drift. Data from subject 3 is less affected by this flaw. The data for subject 1 shows more statistical significance and physical meaning. This dataset was collected after slightly amending the experimental method, where a 6-DOF IMU was changed for a 9-DOF IMU, compensating for the sensor drift with the addition of a magnetometer. Repeating measurements would have provided better data for subjects 2 and 3, however, due to time and COVID-19 restrictions, this was not possible. Despite these errors, results show that a system can be identified given a torque input. While the values for subject 2 and 3 are less physically meaningful, it seems possible to experimentally deduce values by tuning an output to a given input, confirming our hypothesis that residual impedance can be modelled.

Overall, the results support our hypothesis that un-modelled impedance can be mathematically modelled given the relevant parameters. These parameters can be used in the future to tune a zero-impedance control system for an adaptive control tailored to the user. Further experiments can be designed to assess the improvement of the assistive strategy when tuned to the identified parameters.

4.2 Conclusion and further work

A parametric identification method is proposed to tune the gains of a zero-impedance assistive strategy based on factors proper to the user and his exoskeleton. Using the impedance parameters identified in the experiments, and without any knowledge of the impedance of the system, coupled parameters describing the remaining position mismatch can be deduced with the developed experimental procedure. This method was evaluated with experiments on three subjects, which show that unknown human-exoskeleton behaviour can be mathematically modelled by identifying coupled impedance parameters. This framework is uncomplicated yet robust, and can be extended to more daily life activities. Future work includes developing a separate control system which would actively compensate resistance arising from the unknown impedance.

To fully tackle the initial aims, experimental steps would be needed to find a method to improve the controller without considering the IMU feedback giving the knee angle. Using the identified parameters and sEMG signals, an additional controller could be designed, addressing the torque mismatch remaining due to unknown factors. It would then need to be compared to the current zero-impedance control.

In [15] and [43], a similar approach to impedance reduction was taken, adjusting the impedance using ground force reaction as a gait phase detection method. It was shown that the human effort was significantly decreased when the wearers were assisted with the proposed active impedance control strategy. However, it was also noted that the remaining human-orthosis impedance was compensated in different ratios during the swing phase. If using a sEMG based method, the system response could vary based on the current torque input both from the exoskeleton and the human. This approach would benefit of an advanced prediction of human behaviour and allow for control feedback in advance of the motion, giving an advantage over sensorless approaches such as nonlinear disturbance observers.

However, a successful outcome relies on the accuracy of the sensors. Sensor position, calibration, and other factors can influence results. Future work on reducing the number of sensors without compromising performance would add to the robustness and reduce hardware requirements of the exoskeleton. Another factor to consider would be that impedance parameters do not remain constant throughout motion, as assumed in this report. Optimising the parameters online would allow to deal with this and events such as subject fatigue, which the constant parameters fail to take into account.

Bibliography

- [1] T. Sheridan, “Human-Robot Interaction: Status and Challenges,” *Human factors*, vol. 58, Jan. 2016. DOI: 10.1177/0018720816644364.
- [2] D. Pamungkas, W. Caesarendra, H. Soebakti, R. Analia, and S. Susanto, “Overview: Types of Lower Limb Exoskeletons,” *Electronics*, vol. 8, p. 1283, Jan. 2019. DOI: 10.3390/electronics8111283.
- [3] M. Ersen, E. Oztop, and S. Sariel, “Cognition-Enabled Robot Manipulation in Human Environments: Requirements, Recent Work, and Open Problems,” *IEEE Robotics Automation Magazine*, vol. 24, no. 3, pp. 108–122, 2017. DOI: 10.1109/MRA.2016.2616538.
- [4] S. Honig and T. Oron-Gilad, “Understanding and Resolving Failures in Human-Robot Interaction: Literature Review and Model Development,” *Frontiers in Psychology*, vol. 9, p. 861, 2018, ISSN: 1664-1078. DOI: 10.3389/fpsyg.2018.00861. [Online]. Available: <https://www.frontiersin.org/article/10.3389/fpsyg.2018.00861>.
- [5] A. J. Veale and S. Q. Xie, “Towards compliant and wearable robotic orthoses: A review of current and emerging actuator technologies,” *Medical Engineering & Physics*, vol. 38, no. 4, pp. 317–325, 2016, ISSN: 1350-4533. DOI: <https://doi.org/10.1016/j.medengphy.2016.01.010>. [Online]. Available: <http://www.sciencedirect.com/science/article/pii/S135045331600031X>.
- [6] L. Bi, A. . . . Feleke, and C. Guan, “A review on EMG-based motor intention prediction of continuous human upper limb motion for human-robot collaboration,” *Biomedical Signal Processing and Control*, vol. 51, pp. 113–127, 2019, ISSN: 1746-8094. DOI: <https://doi.org/10.1016/j.bspc.2019.02.011>. [Online]. Available: <https://www.sciencedirect.com/science/article/pii/S1746809419300473>.
- [7] T. Yan, M. Cempini, C. M. Oddo, and N. Vitiello, “Review of assistive strategies in powered lower-limb orthoses and exoskeletons,” *Robotics and Autonomous Systems*, vol. 64, pp. 120–136, Feb. 2015, ISSN: 09218890. DOI: 10.1016/j.robot.2014.09.032.
- [8] A. Tsukahara, R. Kawanishi, Y. Hasegawa, and Y. Sankai, “Sit-to-Stand and Stand-to-Sit Transfer Support for Complete Paraplegic Patients with Robot Suit HAL,” *Advanced Robotics*, vol. 24, no. 11, pp. 1615–1638, Jan. 2010, ISSN: 0169-1864. DOI: 10.1163/016918610X512622. [Online]. Available: <https://doi.org/10.1163/016918610X512622>.
- [9] T. Matsubara, A. Uchikata, and J. Morimoto, “Full-body exoskeleton robot control for walking assistance by style-phase adaptive pattern generation,” *2012 IEEE/RSJ International Conference on Intelligent Robots and Systems*, pp. 3914–3920, 2012.
- [10] H. He and K. Kiguchi, “A Study on EMG-Based Control of Exoskeleton Robots for Human Lower-limb Motion Assist,” in *2007 6th International Special Topic Conference on Information Technology Applications in Biomedicine*, 2007, pp. 292–295. DOI: 10.1109/ITAB.2007.4407405.

- [11] A. B. Zoss, H. Kazerooni, and A. Chu, “Biomechanical design of the Berkeley lower extremity exoskeleton (BLEEX),” *IEEE/ASME Transactions on Mechatronics*, vol. 11, no. 2, pp. 128–138, 2006, ISSN: 1941-014X. DOI: 10.1109/TMECH.2006.871087.
- [12] E. Guizzo and H. Goldstein, “The rise of the body bots [robotic exoskeletons],” *IEEE Spectrum*, vol. 42, no. 10, pp. 50–56, Oct. 2005, ISSN: 1939-9340. DOI: 10.1109/MSPEC.2005.1515961.
- [13] Z. Yang, Y. Zhu, X. Yang, and Y. Zhang, “Impedance Control of Exoskeleton Suit Based on Adaptive RBF Neural Network,” in *2009 International Conference on Intelligent Human-Machine Systems and Cybernetics*, vol. 1, 2009, pp. 182–187. DOI: 10.1109/IHMSC.2009.54.
- [14] K. Hornik, M. Stinchcombe, and H. White, “Multilayer feedforward networks are universal approximators,” *Neural Networks*, vol. 2, no. 5, pp. 359–366, 1989, ISSN: 0893-6080. DOI: [https://doi.org/10.1016/0893-6080\(89\)90020-8](https://doi.org/10.1016/0893-6080(89)90020-8). [Online]. Available: <http://www.sciencedirect.com/science/article/pii/0893608089900208>.
- [15] F. Wehbi, W. Huo, M. el Rafei, M. Khalil, and S. Mohammed, “Active impedance control of a knee-joint orthosis during swing phase,” in *IEEE ... International Conference on Rehabilitation Robotics : [proceedings]*, vol. 2017, Jun. 2017, pp. 435–440. DOI: 10.1109/ICORR.2017.8009286.
- [16] C. Gaz, F. Flacco, and A. D. Luca, “Identifying the dynamic model used by the KUKA LWR: A reverse engineering approach,” in *2014 IEEE International Conference on Robotics and Automation (ICRA)*, 2014, pp. 1386–1392, ISBN: 1050-4729. DOI: 10.1109/ICRA.2014.6907033.
- [17] D. Farina and F. Negro, “Accessing the Neural Drive to Muscle and Translation to Neurorehabilitation Technologies,” *IEEE Reviews in Biomedical Engineering*, vol. 5, pp. 3–14, 2012. DOI: 10.1109/RBME.2012.2183586.
- [18] D. Winter, “Biomechanics and Motor Control of Human Movement, Fourth Edition,” Jun. 2009. DOI: 10.1002/9780470549148.ch5.
- [19] L.-N. Tong, Z.-G. Hou, L. Peng, W. Wang, Y.-X. Chen, and M. Tan, “Multi-channel sEMG time series analysis based human motion recognition method,” *Zidonghua Xuebao/Acta Automatica Sinica*, vol. 40, pp. 810–821, Jun. 2014. DOI: 10.3724/SP.J.1004.2014.00810.
- [20] K. Kiguchi and Y. Hayashi, “An EMG-Based Control for an Upper-Limb Power-Assist Exoskeleton Robot,” *IEEE Transactions on Systems, Man, and Cybernetics, Part B (Cybernetics)*, vol. 42, no. 4, pp. 1064–1071, 2012. DOI: 10.1109/TSMCB.2012.2185843.
- [21] A. J. Young, H. Gannon, and D. P. Ferris, “A Biomechanical Comparison of Proportional Electromyography Control to Biological Torque Control Using a Powered Hip Exoskeleton,” eng, *Frontiers in bioengineering and biotechnology*, vol. 5, p. 37, Jun. 2017, ISSN: 2296-4185. DOI: 10.3389/fbioe.2017.00037. [Online]. Available: <https://pubmed.ncbi.nlm.nih.gov/28713810%20https://www.ncbi.nlm.nih.gov/pmc/articles/PMC5491916/>.
- [22] M. Gandolla, E. Guanziroli, A. D’Angelo, G. Cannaviello, F. Molteni, and A. Pedrocchi, “Automatic Setting Procedure for Exoskeleton-Assisted Overground Gait: Proof of Concept on Stroke Population,” eng, *Frontiers in neurorobotics*, vol. 12, p. 10, Mar. 2018, ISSN: 1662-5218. DOI: 10.3389/fnbot.2018.00010. [Online]. Available: <https://pubmed.ncbi.nlm.nih.gov/29615890%20https://www.ncbi.nlm.nih.gov/pmc/articles/PMC5868134/>.

- [23] G. Durandau, D. Farina, G. Asín-Prieto, I. Dimbwadyo-Terrer, S. Lerma-Lara, J. L. Pons, J. C. Moreno, and M. Sartori, “Voluntary control of wearable robotic exoskeletons by patients with paresis via neuromechanical modeling,” eng, *Journal of neuroengineering and rehabilitation*, vol. 16, no. 1, p. 91, Jul. 2019, ISSN: 1743-0003. DOI: 10.1186/s12984-019-0559-z. [Online]. Available: <https://pubmed.ncbi.nlm.nih.gov/31315633/>
- [24] R. H. Chowdhury, M. B. I. Reaz, M. A. B. M. Ali, A. A. A. Bakar, K. Chellappan, and T. G. Chang, “Surface electromyography signal processing and classification techniques,” eng, *Sensors (Basel, Switzerland)*, vol. 13, no. 9, pp. 12 431–12 466, Sep. 2013, ISSN: 1424-8220. DOI: 10.3390/s130912431. [Online]. Available: <https://pubmed.ncbi.nlm.nih.gov/24048337/>
- [25] C. Fleischer, C. Reinicke, and G. Hommel, “Predicting the intended motion with EMG signals for an exoskeleton orthosis controller,” in *2005 IEEE/RSJ International Conference on Intelligent Robots and Systems*, 2005, pp. 2029–2034. DOI: 10.1109/IROS.2005.1545504.
- [26] C. Caulcrick, W. Huo, and R. Vaidyanathan, “Human Joint Torque Modelling with MMG and EMG during Lower Limb Human-Exoskeleton Interaction,” Tech. Rep. [Online]. Available: https://github.com/cic12/ieee_appx.
- [27] C. ; Caulcrick, W. ; Huo, E. ; Franco, S. ; Mohammed, W. ; Hoult, R. Vaidyanathan, C. Caulcrick, W. Huo, E. Franco, S. Mohammed, and W. Hoult, “Model Predictive Control for Human-Centred Lower Limb Robotic Assistance IEEE Transactions on Medical Robotics and Bionics IEEE TRANSACTIONS ON MEDICAL ROBOTICS AND BIONICS 1 Model Predictive Control for Human-Centred Lower Limb Robotic Assistance,” Tech. Rep.
- [28] G. Yin, X. Zhang, D. Chen, H. Li, J. Chen, C. Chen, and S. Lemos, “Processing Surface EMG Signals for Exoskeleton Motion Control,” eng, *Frontiers in neurorobotics*, vol. 14, p. 40, Jul. 2020, ISSN: 1662-5218. DOI: 10.3389/fnbot.2020.00040. [Online]. Available: <https://pubmed.ncbi.nlm.nih.gov/32765250/>
- [29] *HEBI Robotics Hardware*. [Online]. Available: <https://docs.hebi.us/hardware.html#modules>.
- [30] Arduino, “Arduino Nano 33 BLE Product Specifications,” Tech. Rep. [Online]. Available: https://content.arduino.cc/assets/Nano_BLE MCU-nRF52840_PS_v1.1.pdf.
- [31] “LSM9DS1 Datasheet,” [Online]. Available: https://content.arduino.cc/assets/Nano_BLE_Sense_lsm9ds1.pdf.
- [32] S. O. H. Madgwick, A. J. L. Harrison, and R. Vaidyanathan, “Estimation of IMU and MARG orientation using a gradient descent algorithm,” in *2011 IEEE International Conference on Rehabilitation Robotics*, 2011, pp. 1–7. DOI: 10.1109/ICORR.2011.5975346.
- [33] *Resample uniform or nonuniform data to new fixed rate - resample polyfit - mathworks united kingdom*. [Online]. Available: <https://uk.mathworks.com/help/signal/ref/resample.html>.
- [34] A. Hof, “The relationship between electromyogram and muscle force,” *Sportverletzung Sportschaden : Organ der Gesellschaft für Orthopädisch-Traumatologische Sportmedizin*, vol. 11, pp. 79–86, Jun. 1997. DOI: 10.1055/s-2007-993372.
- [35] Merletti R, Rau G, Disselhorst-Klug C, Stegeman D.F., and Hägg G.M., *Recommendations for sensor locations on individual muscles*. [Online]. Available: <http://seniam.org/>.

- [36] TMSI, *Porti 7 User Manual*, Oldenzaal, The Netherlands, 2017.
- [37] M. B. I. Raez, M. S. Hussain, and F. Mohd-Yasin, “Techniques of EMG signal analysis: detection, processing, classification and applications,” eng, *Biological procedures online*, vol. 8, pp. 11–35, 2006, ISSN: 1480-9222. DOI: 10.1251/bpo115. [Online]. Available: <https://pubmed.ncbi.nlm.nih.gov/16799694/> [2023-03-15].
- [38] *Polynomial curve fitting - matlab polyfit - mathworks united kingdom*. [Online]. Available: <https://uk.mathworks.com/help/matlab/ref/polyfit.html>.
- [39] P. Heinemann and M. Kasperski, “Damping Induced by Walking and Running,” *Procedia Engineering*, vol. 199, pp. 2826–2831, 2017, ISSN: 1877-7058. DOI: <https://doi.org/10.1016/j.proeng.2017.09.537>. [Online]. Available: <https://www.sciencedirect.com/science/article/pii/S1877705817340481>.
- [40] J. Ahn and N. Hogan, “Walking Is Not Like Reaching: Evidence from Periodic Mechanical Perturbations,” *PloS one*, vol. 7, e31767, Apr. 2012. DOI: 10.1371/journal.pone.0031767.
- [41] *System Identification Overview - Matlab Simulink - Mathworks United Kingdom*. [Online]. Available: <https://uk.mathworks.com/help/ident/gs/about-system-identification.html>.
- [42] *Ensemble methods*. [Online]. Available: <https://scikit-learn.org/stable/modules/ensemble.html>.
- [43] W. Huo, S. Mohammed, and Y. Amirat, “Impedance Reduction Control of a Knee Joint Human-Exoskeleton System,” *IEEE Transactions on Control Systems Technology*, vol. 27, no. 6, pp. 2541–2556, Nov. 2019, ISSN: 1558-0865. DOI: 10.1109/TCST.2018.2865768.